Neuron, Volume 60

Supplemental Data

Similarity Effect and Optimal Control of Multiple-Choice Decision Making

Moran Furman and Xiao-Jing Wang

Supplemental Results

Dependence of neural response during target presentation on the number of targets

In our simulations, increasing the number of targets reduced the neural response during target presentation (Fig 5E). Quantitatively, the mean response of the pyramidal neurons to 2, 4 and 8 targets between t=800ms and 1300ms was 47.0±1.5Hz, 37.9±1.0Hz, and 28.1±0.7Hz respectively. Two factors contribute in our model to the reduction of response when the number of choices is increased. First, we assume that the magnitude of the target input is monotonically decreasing as function of the number of targets, presumably due to a normalization of neural activity in the upstream system where the target-input is encoded. Second, feedback inhibition within the circuit contributes further to the modulation of response as a function of the number of targets. Indeed, the mean response of the inhibitory neurons to 2, 4 and 8 targets was 5.0±0.4Hz, 6.7±0.3Hz, and 9.5±0.2Hz respectively. To differentiate the two factors, we performed a set of simulations where the peak magnitude of the target-input did not depend on the number of targets. The response of the pyramidal neurons to 2, 4 and 8 targets was 46.8±1.5Hz, 45.1±1.0Hz, and 39.1±0.7Hz respectively, and the response of the inhibitory neurons was 5.0±0.4Hz, 7.2±0.3Hz, and 11.0±0.2Hz. Thus, even when the peak magnitude of the target-input does not depend on the number of targets, feedback inhibition reduces the response when the number of targets is increased, but the differences in the pyramidal neuronal responses are relatively small, suggesting that a larger effect is due to the presumed normalization of target-representing input neural activity.

Supplemental Experimental Procedures

Fits to behavioral data

Psychometric curves (Figs 6A, 7E, 8A) were fitted by a Weibull function:

$$\%correct = 1 - (1 - A) \times \exp\left(-(c'/\alpha)^{\beta}\right) \qquad \text{(A1)}$$

where A is the chance level (0.125, 0.25 and 0.5 for 2,4 and 8 choices respectively); c' is the coherence level; α and β are free parameters. Chronometric curves (Figs 6B, 7D, 8B) were fitted by

$$RT = \frac{C}{kc'}\tanh(Ckc') + t_R \qquad \text{(A2)}$$

where c' is the coherence level; C, k and t_R are free parameters.

Data analysis and visualization

To visualize the spatio-temporal dynamics of the network activity (Figs 3B and 4), spike data was first smoothed using a sliding window both in time (40ms window, 10ms time step) and in space (40 neurons). The resulting firing rates were color encoded.
The activity of neurons located around the targets (Figs 3C, 5 and 7) was calculated by averaging the activity of 40 neurons around each of the targets, and smoothing it using a temporal sliding window of 80ms advanced at 5ms time steps.

To estimate activity buildup rates during decision formation (Fig. 5D), we first constructed a peri-stimulus time histogram (10ms bins) averaged over 40 neurons around each of the targets. The buildup rate is the slope of a linear fit to the firing-rates during 1580-1700ms.

Decision readout

Response time and decision outcome were determined as follows. Every 5ms, a spike count was performed over a 100ms window and smoothed spatially using a sliding window of 20 neurons. Decision was reached when any of the resulting firing-rates crossed a threshold of 60Hz. The selected target was determined as the one closest to the population vector (Georgopoulos et al., 1982)

$$\theta_P(t) = \arctan\left(\frac{\sum_{i=1}^{N_E} r_i \sin(\theta_i)}{\sum_{i=1}^{N_E} r_i \cos(\theta_i)}\right) \qquad \text{(A3)}$$

where i runs over the population of pyramidal neurons, each with preferred direction θ_i and activity r_i.

In some trials, merging of activity around adjacent targets was observed (Fig. 7). To quantify this phenomenon, we calculated the average activity of 40 neurons located around each of the targets at a 100ms time window around the time when the threshold of 60Hz was crossed. If more than one of these neural groups crossed a 30Hz activity level, activity merging was considered to take place.

The response time RT was calculated by

$$RT = t_D - t_{start} + t_{post} \qquad \text{(A4)}$$

where t_D is the time at which decision is reached, defined as the mid-point of the time window when the threshold was crossed; $t_{start} = 1300ms$ is onset of the motion stimulus; and $t_{post} = 80ms$ is the post-decision time due to execution of the saccadic eye movement.

Reward rate

The reward rate R is defined by $R = P/T$ where P is the performance (average fraction of correct choices) and T is the average trial duration. The performance is calculated according to (Gold and Shadlen, 2002; Lo and Wang, 2006)

$$P = \sum_{k=1}^{N_{coh}} n_k p_k \quad \text{(A5)}$$

where k runs over the different coherence levels, n_k is the percentage of trials with the coherence level k, and p_k is the fraction of correct choices. The average trial time T is

$$T = \sum_{k=1}^{N_{coh}} n_k \left[p_k (RT_k^{correct} + t_{ITI}) + (1 - p_k)(RT_k^{error} + t_{ITI} + t_{penal}) \right] \quad \text{(A6)}$$

where $RT_k^{correct}$ and RT_k^{error} are the average response times in correct and error trials, respectively, for the coherence level k; $t_{ITI} = 1000ms$ is the inter-trial-interval, and $t_{penal} = 1000ms$ is a penalty time added after an error trial.

Numerical integration

Numerical integration was performed using a modified RK2 algorithm with firing-time interpolation (Hansel et al., 1998), with integration time step of $\Delta t = 0.02ms$.

Supplemental Figures

Figure S1

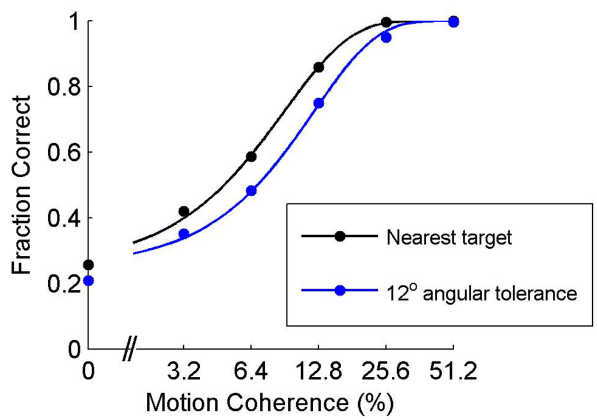

Figure S1: Simulated performance in the 4-choice task using two different readout algorithms: Selecting the target nearest the population vector at the time of threshold crossing (black), and selecting a target if it falls within 12° tolerance from the population vector (blue). Performance is somewhat lower with the latter algorithm due to the fraction of trials where the tolerance criterion is not met (and therefore considered error trials).

Figure S2

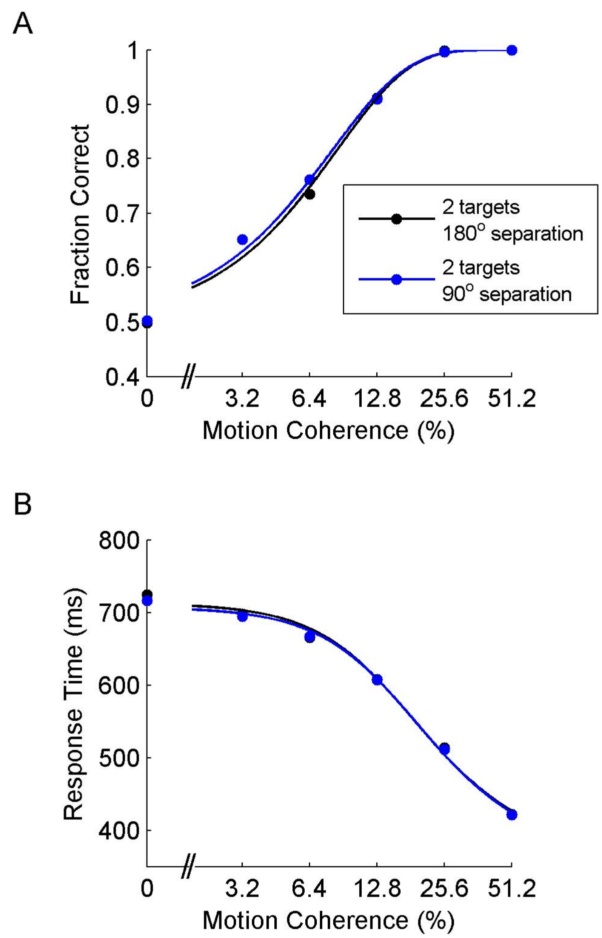

Figure S2: Simulated behavioral data for 2-choice tasks with 90^o and 180^o angular separation between the targets. Performance (A) and mean response times on correct trials (B) as a function of motion coherence. The control signal in these simulations was 6Hz. Both performance and response times were identical in the two conditions.

Figure S3

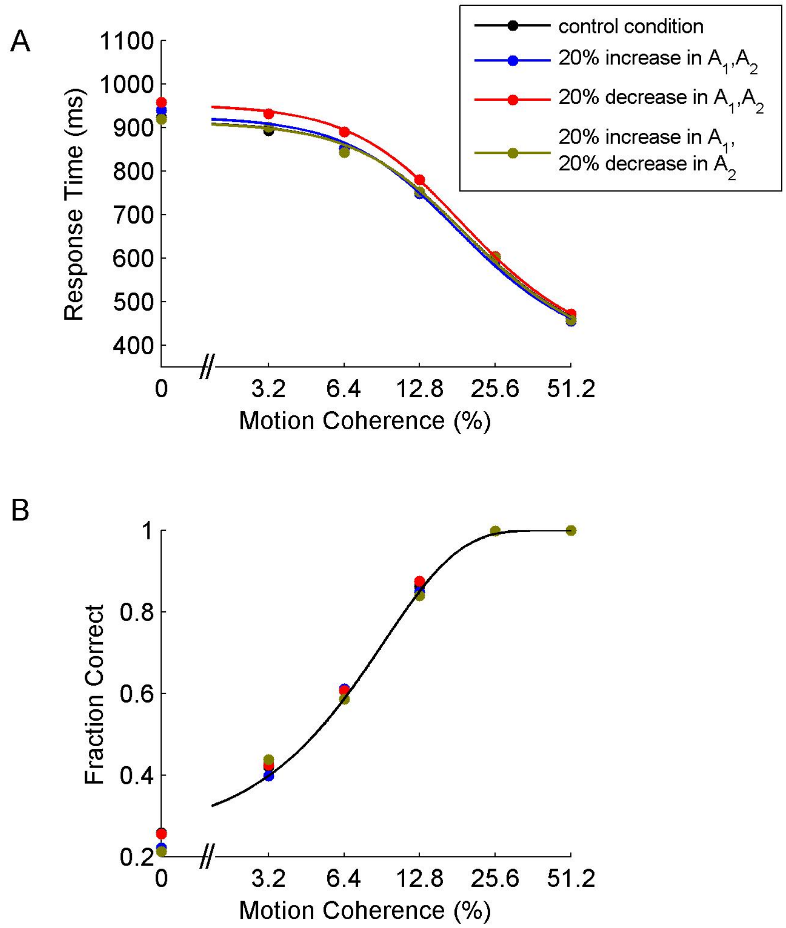

Figure S3: Robustness of the decision result to changes in the magnitude of the target-input before the onset of the motion stimulus. Response times (A) and performance (B) under different parameter combinations (see Experimental Procedures): Control condition (black), 20% increase in A_1 and A_2 (blue), 20% decrease in A_1 and A_2 (red), and 20% increase in A_1 along with 20% decrease in A_2 (green).

REFERENCES

Georgopoulos, A.P., Kalaska, J.F., Caminiti, R., and Massey, J.T. (1982). On the relations between the direction of two-dimensional arm movements and cell discharge in primate motor cortex. Journal of Neuroscience *2*, 1527-1537.

Gold, J.I., and Shadlen, M.N. (2002). Banburismus and the brain: Decoding the relationship between sensory stimuli, decisions, and reward. Neuron *36*, 299-308.

Hansel, D., Mato, G., Meunier, C., and Neltner, L. (1998). On numerical simulations of integrate-and-fire neural networks. Neural Computation *10*, 467-483.

Lo, C.-C., and Wang, X.-J. (2006). Cortico–basal ganglia circuit mechanism for a decision threshold in reaction time tasks. Nature Neuroscience *9*, 956-963.